ENERGY FLEXIBILITY FROM INDUSTRIAL SUPPLY SYSTEMS BASED ON DIFFERENT OPTIMIZATION HORIZONS – AN APPLICATION TO A GERMAN MANUFACTURING INDUSTRY

Johannes B. Lipka*[,1,2], Lukas Höttecke[1], Paul Stursberg[1], Michael Metzger[1], Martin Kautz[1], Hans Jörg Heger[1], Stefan Niessen[1,2]

[1]Siemens Technology, Sustainable Energy & Infrastructure, Munich, Germany

[2]Technical University of Darmstadt, The Technology and Economics of Multimodal Energy Systems Lab, Darmstadt, Germany

*Corresponding Author: johannes-bernd.lipka@siemens.com

ABSTRACT

The manufacturing industry faces challenges in decarbonizing its facilities to align with environmental goals. Flexibility plays a key role in the decarbonization strategies due to the intermittent nature of the renewable energy sources wind and solar. Assessing investment decisions in the context of decarbonization requires accurate simulations to estimate the benefits of each decarbonization decision, particularly the value of different flexibility resources in each energy system design variant. This value can change substantially depending on the dispatch strategy in use, and particularly the optimization horizon. Furthermore, distinct energy system configurations, flexibility sources, or energy tariff structures may exhibit disparate sensitivities to different optimization horizons. To quantify this dependency, this study investigates the flexibility of a multi-modal energy system based on a real manufacturing factory in Germany, utilizing a lithium-ion battery, cold and hot water storage units as flexibility sources. The unit commitment problem is modeled as a Mixed Integer Linear Program (MILP), and four dispatch strategies with different optimization horizons (one year, 24 hours, 12 hours, and 1 hour) are employed. Five commonly used energy tariff structures, with and without a monthly peak-load component, are considered. Results indicate that the optimization horizon strongly influences the system's trajectory and key performance indicators (KPIs). Results show, that depending on the optimization horizon and energy tariff, OPEX savings and customer KPIs can significantly vary. For example, choosing a shorter optimization horizon can lead to a 7.5% increase in OPEX savings from flexibility sources, 80% increase in projected CO_2 emissions from gas purchase, affect various system components, such as battery usage (leads to more than 90% reduced full storage cycles), energy from the power grid, and PV curtailment. The research emphasizes the need for accurate cost estimation for time-varying tariffs and peak demand charges, considering real-world controllers' limited foresight. The results aim to assist decision-makers in prioritizing system components for in-depth analysis.

1 INTRODUCTION

The most recent empirical data (2022) indicates that the German manufacturing industry sector accounts for approximately 28% of the annual national energy consumption (around 2368TWh in 2022). However, only 6.3% of this consumption is derived from renewable energy sources (AGEB, 2023), thereby positioning the sector as a significant contributor to carbon emissions. Escalating energy costs, carbon-emission levies, and newly established national objectives for achieving greenhouse neutrality by 2045 (Umwelt-Bundesamt, 2023), have prompted industries to allocate substantial investments towards the development and implementation of novel decarbonization strategies for their manufacturing facilities. Given the intermittent nature of wind and solar, energy flexibility assumes a pivotal role in these decarbonization strategies. Effectively harnessing a site's energy flexibility sources has the potential to markedly reduce its Operational Expenditure (OPEX). The implementation of most decarbonization strategies necessitates considerable financial commitments, underscoring the

https://doi.org/10.52202/077185-0159

importance of accurate simulations to assess the anticipated benefits of each decarbonization decision. This includes a comprehensive evaluation of the value associated with energy flexibility within the framework of each energy system design.

The benefits obtained by a site's energy flexibility sources can be influenced by a variety of factors. Principal among these considerations are the intrinsic characteristics of the flexibility, the configuration of the energy system, and economic inducements, particularly in terms of energy procurement tariff structures. An often overlooked yet pivotal determinant in this context is the dispatch strategy employed or to be employed within the onsite energy system. Our assumption is that the combined impact of these diverse factors and their ensuing advantages is notably influenced by the selected dispatch strategy of the site. The evolution of intelligent sensor and actuator technologies has precipitated the adoption of predictive dispatch methodologies, exemplified by Model Predictive Control (MPC) or commonly referred to as Rolling Horizon Control (RHC), within the domain of industrial energy systems. Based on the available forecasts and control capabilities, those predictive dispatch strategies have different optimization horizons that exert significant influence on the anticipated gains and benefits. This research quantifies this influence and points out the key aspects of the energy system that are most influenced by the choice of the optimization horizon.

1.1 Relevant Work and Literature Review

The unit commitment problem is primarily concerned with determining the optimal operation of resources within an energy system. Various dispatch strategies, such as the load following strategy (Gupta *et al*., 2010), cycle charging strategy (Ma *et al*., 2022) and combined dispatch strategy (Shezan *et al*., 2022) have been investigated. Nevertheless, the aforementioned strategies do not capitalize on any available future information. Model Predictive Control (MPC) is a group of control strategies that can leverage future information or forecasts to optimize the integration of RES and the utilization of flexibility sources within an energy system, i.e., using a rolling horizon (RH) principle. MPC employs a mathematical model to predict the system's future trajectory based on forecasted energy demands, energy prices, and weather conditions. Subsequently, the unit commitment problem is optimized for a specified number of future steps. Extensive research on MPC dispatch strategies has been conducted on multiple types of energy systems, such as islanded microgrids (Hans, 2021), (Moretti et al., 2019) (where primary source of flexibility was offered by energy storage units (ESUs)), grid connected microgrids with multiple stakeholders (Alarcón *et al*., 2022), commercial buildings with HVAC systems (Ma *et al*., 2012) and thermal energy storages (Cole *et al*., 2012).

Research on industrial sites also mainly focuses on operational optimization issues (Xu *et al*., 2021). Mitra *et al*. (2013) built a MILP model of a CHP plant and optimized its dispatch over the curse of one week achieving financial gains between 5% and 20%. Similar work was done by Bischi *et al*. (2019), where an MPC optimized the use of CHP units of an energy system with electric, high and low temperature thermal energy needs. Agha *et al*. (2010) considered an industrial site with a power generating unit and a manufacturing unit. Using a MILP formulation, and accounting for flexibilities on both sides, the authors managed to optimize manufacturing scheduling as well as the power generation thus effectively optimizing the energy efficiency of the whole industrial site. Regarding the optimization horizon, a few papers have investigated trade-offs between computational costs and controller performance. Zhao *et al*. (2018) investigated the impact of the control horizon in a trajectory based MPC that controls a complex steam-water loop process on ships. Increasing the control horizon increased the system's performance but made the optimization problem less tractable. Sawma *et al*. (2018) proved under which conditions, the use of a prediction horizon equal to one in first-order linear systems yields similar results to prediction horizons greater than one. However, the proof only regarded trajectory based and not economic MPCs. Schreck (2016) explored how the time resolution used in a model affects both the computation time and the accuracy of results in solving a rolling horizon problem. Pérez-Piñeiro and Boyd (2023) investigated the difference of anticipated savings when controlling a simple grid with a perfect dispatcher and an MPC. None of the above papers investigate the synergies between optimization horizon, projected financial wins and available energy flexibility sources.

https://doi.org/10.52202/077185-0159

1.2 Contributions

This research investigates the effects of different optimization horizons of industrial energy system dispatch algorithms across different archetypical system setups with respect to different flexibility sources and energy tariff structures. This analysis proves beneficial for system designers and decision-makers on two fronts. Firstly, since the selection of the optimization horizon is closely tied to the capabilities of the existing installed configuration (site's energy system design, available controllers, sensors, and actuators), a more precise estimation of the benefits of a flexibility source necessitates consideration of the employed optimization horizon. Secondly, in the context of future energy system design sizing optimizations, where perfect foresight is typically assumed, the study outlines which components are most susceptible to optimization horizon influence, providing valuable insights for designers to anticipate system behaviour and crucial design considerations. Moreover, the study illustrates how smart predictive control of systems with diverse optimization horizons can serve as an additional source of financial gains in future investment decisions. Subsequently, this research has following contributions:

1. Provide a quantitative comparison between different optimization horizons and document the key aspects of energy OPEX of the industrial system that are most influenced.
2. Showcase how considering an optimization horizon for the unit commitment problem, that does not adhere to the stakeholder's current control capabilities, may mislead investment decisions.
3. Achieve the aforementioned, using a simplified aggregated energy system design based on a real design, using real energy load and price data as well as relevant stakeholder KPIs.

2 Simulation Set-Up, Parameters and Assumptions

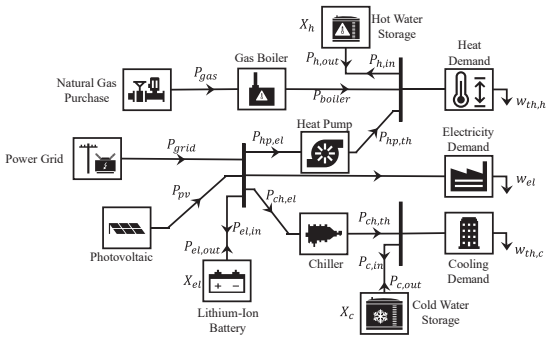

Figure 1: Power Flow System Model

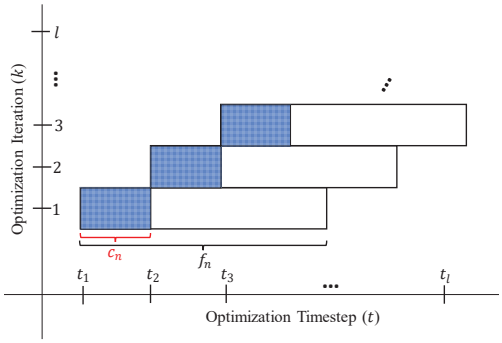

Figure 2: Rolling Horizon Approach

Consider the system depicted in Figure 1, and the set of its assets $I = [gas, grid, pv, el, boiler, h, c, ch, hp]$. Here, the abbreviations el, h, c, ch, hp refer to the lithium-ion battery, hot water storage, cold water storage, chiller and heat-pump, respectively. The installed power p_i^{rPower} and capacity $x_i^{rCapacity}$ of the assets, $\forall\, i \in I$, is considered fixed and the corresponding power flows are denoted by $P = \{P_i, \forall\, i \in I\}$, e.g, $P_{hp,th}$ is the thermal power flow of the heat pump. $w_{th,h}, w_{el}, w_{th,c}$ refer to the heat, electric and cooling demand respectively. X_{el}, X_h, X_c describe the stage of charge (SOC) of the lithium-ion battery, and the thermal energy levels of the hot and cold water storages. A more detailed description of the system's parameters and workflow is given in Section 2.2, whereas meaning of symbols, subscripts and arguments can be further found in the nomenclature. Given the dispatcher's forecast horizon f_n and control horizon c_n, at each optimization iteration k, the MPC will solve the unit commitment problem for f_n future steps out of which only the first c_n steps will be applied to our system and then the problem will be resolved with the new initial conditions and forecasts (see Figure 2). To mitigate the influence of forecast errors, the forecasted values are regarded as perfect, namely forecast error is zero. Section 2.1 describes the mathematical problem that is solved.

https://doi.org/10.52202/077185-0159

2.1 Mathematical Formulation

In this work, decision variables and optimization costs are denoted with capital letters, whereas parameters and constants with small letters. The following cost function is minimized at each optimization iteration k:

$$\min_{P} Z^{OPEX}(k) \;=\; \min_{P} Z^{OPEX_{energy}}(k) + Z^{OPEX_{mPeak}}(k) \tag{1}$$

where $Z^{OPEX_{energy}}(k)$ refers to the operating costs of energy procurement and is equivalent to

$$Z^{OPEX_{energy}}(k) \;=\; \sum_{t=t_k}^{t_k+f_n} Z_t^{OPEX_{energy}} \;=\; \sum_{t=t_k}^{t_k+f_n} om_{grid}(t) \times P_{grid}(t) + om_{gas}(t) \times P_{gas}(t) \tag{2}$$

Power Input/Output Constraint
All power flows, i.e., $\forall P_i \in P$ must be constrained as follows:

$$0 \leq\; P_i \leq p_i^{rPower}. \tag{3}$$

Storage Dynamics Constraint
For each storage $i \in [el, c, h]$, with a charge-discharge binary status $\delta_i(t)$ following must hold:

$$0 \leq\; X_i(t) \leq x_i^{rCapacity} \tag{4}$$

$$X_i(\mathrm{t}+1) \;=\; (1-\eta_i^{Self}) \times X_i(\mathrm{t}) \;+\; \eta_i^{Ch} \times P_{i,in}(\mathrm{t}) \;-\frac{1}{\eta_i^{Dch}} P_{i,out}(\mathrm{t}) \tag{5}$$

$$P_{i,in}(t) \leq p_i^{rPower} \times \delta_i(t) \tag{6}$$

$$P_{i,out}(t) \leq p_i^{rPower} \times (1-\delta_i(t)), \tag{7}$$

where $\eta_i^{Self}, \eta_i^{Ch}, \eta_i^{Dch}$ the self-discharge, charge and discharge efficiencies. Furthermore, consider $\mathrm{t}_{k,initial}, \mathrm{t}_{k,final}$ as the first and final timestep of optimization iteration k. By using a slack variable (8), we can define a (dis)charging incentive/cost for the storages (9) and add it to our energy OPEX (10).

$$V_i(\mathrm{k}) = X_i(\mathrm{t}_{k,final}) - X_i(\mathrm{t}_{k,initial}), \forall\, i \in [el, c, h] \tag{8}$$

$$Z_{(dis)charg.Inc.}^{OPEX_{energy}}(i,k) \;>=\; -0.01 * V_i(\mathrm{k})\; \forall\, i \in [el, c, h] \tag{9}$$

$$\mathrm{Z}_{\mathrm{new}}^{OPEX_{energy}}(k) \;= Z^{OPEX_{energy}}(k) \;+ \sum_{i \in [el,c,h]} Z_{(dis)charg.Inc.}^{OPEX_{energy}}(i,k) \tag{10}$$

Constraints (8), (9) model a charging incentive and discharging cost of 0.01€ per kWh. This incentivizes dispatchers with limited foresight to charge the battery when adequate PV is available that otherwise would be curtailed. Additionally, the storages are not discharged unless the required energy not sourced from the storage is more expensive than 0.01€ per kWh.

Available Renewable Energy Constraint
Given the maximum normed available PV power $v_{pv}(t)$ at timestep t, output $P_{pv}(t)$ is constrained by

$$0 \leq\; P_{pv}(t) \leq v_{pv}(t) \times p_{pv}^{rPower} \tag{11}$$

https://doi.org/10.52202/077185-0159

Energy Conversion Constraint
Power outputs of energy converters are governed by their efficiencies. We regard constant efficiency for the chiller and boiler and a time variant coefficient of performance (COP) for the heat pump, thus following holds:

$$P_{boiler}(t) = \eta^{in}_{boiler} \times P_{gas}(t) \tag{12}$$

$$P_{ch,th}(t) = \eta^{in}_{chiller} \times P_{ch,el}(t) \tag{13}$$

$$P_{hp,th}(t) = \eta^{in}_{hp}(t) \times P_{hp,el}(t) \tag{14}$$

Power Equilibrium
Thermal and electric load must be met at all times.

$$P_{h,out}(t) + P_{boiler}(t) + P_{hp,th}(t) = w_{th,h}(t) + P_{h,in}(t) \tag{15}$$

$$P_{grid}(t) + P_{pv}(t) + P_{el,out}(t) = w_{el}(t) + P_{el,in}(t) + P_{hp,el}(t) + P_{ch,el}(t) \tag{16}$$

$$P_{ch,th}(t) + P_{c,out}(t) = w_{th,c}(t) + P_{c,in}(t) \tag{17}$$

Monthly Peak Load
Unless the perfect dispatcher is used (see next section), all other dispatchers that have limited foresight need a heuristic rule to predict each month's peak load. This can become a difficult task due to the various data (weather, load, disturbances, energy prices) that need to be accurately known for the whole billing period (Cole *et al*., 2012). We use the following heuristic rule. In case of a monthly peak load component in the energy procurement tariff, the term $Z^{OPEX_{mPeak}} \neq 0$ describes the relevant costs.

$$Z^{OPEX_{mPeak}}(k) = \sum_{m=m_k}^{f_m} Z_m^{OPEX_{mPeak}} = \sum_{m=1}^{f_m} om_{mPeak} \times P_{grid,max}(m) \times l(k,m), \tag{18}$$

where f_m the months entailed in the optimization horizon, om_{mPeak} the monthly peak load cost per kW and $P_{grid,max}(m)$ the maximum value of the grid usage in this month. However, the value of $P_{grid,max}(m)$ cannot be known a priori and is thus approximated at each iteration. Let $\tilde{p}^{max}_{grid}$ be our first rough guess for the optimization's first month's peak load. Then for each month m entailed in the optimization horizon we define the decision variable $P_{grid,max}(m)$ that is constrained as follows:

$$P_{grid,max}(m) \geq \tilde{p}^{max}_{grid} \tag{19}$$

$$P_{grid}(t) \leq P_{grid,max}(m) \; \forall t \in m \tag{20}$$

At each optimization timestep, the value of $\tilde{p}^{max}_{grid}$ is updated as follows. If the month hasn't changed, then the new value of $\tilde{p}^{max}_{grid}$ is

$$\tilde{p}^{max}_{grid_{new}} = max(\tilde{p}^{max}_{grid}, P_{grid,max}(m)). \tag{21}$$

Due to seasonal fluctuations, there may be different monthly target peaks over the course of the year. In the context of adaptive peak estimation, it is important to recalibrate the initial guess value for the forthcoming month's peak whenever transitioning to a new month. Thus, if the month changes then

$$\tilde{p}^{max}_{grid_{new}} = \beta \times \tilde{p}^{max}_{grid}, \tag{22}$$

where β a user-defined parameter. For the selected use case, $\beta = 0.8$ is chosen. The weight $l(t,m)$ is time-dependent and is used to regulate the influence of the cost term $Z^{OPEX_{mPeak}}(k)$ in our optimization

https://doi.org/10.52202/077185-0159

problem. At the start of the month, an increase of $P_{grid,max}(m)$ may lead to greater demand costs but will also allow greater future grid flexibility, as for the rest of the month, the controller will be able to use the grid more at no additional cost. However, as the end of the month approaches, the additional benefits of increasing $P_{grid,max}(m)$ diminish and any additional increase will only lead to greater OPEX costs. Thus, given $a(m)$ the number of timesteps of month m, f_n the number of forecast timesteps and k_m the current optimization iteration starting from the start of the month, we define

$$l(k,m) = a(m)^{(-max(a(m)-f_n-k_m,\ 1)/a(m))}. \tag{23}$$

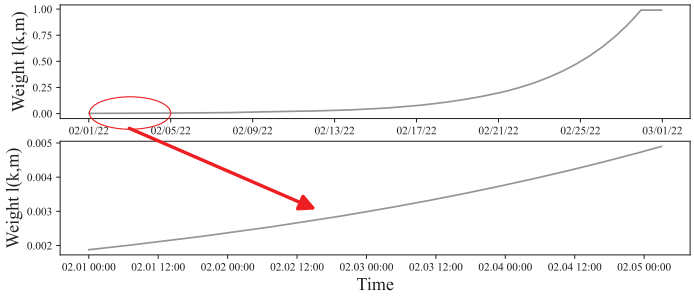

Figure 3: Example progression of weight $l(k,m)$ for the month of February.

For example, for the month of February ($m = 2$), with a time resolution of 1 hour, forecast horizon of 12 hours, control horizon of 1 hour, and current optimization iteration starting on February 2nd at 12p.m, then $a(2) = 672$, $f_n = 12$, and $k_m = 36$ (24 from 1st February plus 12). Figure 3 depicts the respective weight for whole of February. It is easy to see, that increments of $P_{grid,max}(m)$ at the start of the month are weighted less than increments at the end of the month. It is crucial to emphasize that while this heuristic yields good, indicative, and realistic results, it does not assert itself as the optimal solution by any means. It is not the focus of this paper to propose the optimal heuristic.

2.2 Model Description

The following section describes the model and parameters employed during the simulation. In adherence to customer confidentiality and for the sake of simplification, the model has been aggregated. Consequently, certain processes and energy flows have been omitted, while certain parameters have been adjusted or rounded. The model encompasses four distinct energy flows, specifically the flows of electrical, chemical, and thermal energies. The thermal energy flow is further subdivided into two categories: thermal energy allocated for the site's hot water requirements and thermal energy designated for the site's cold-water requirements. Figure 4 displays the electrical $w_{el}(t)$, heat $w_{th,h}(t)$ and cooling $w_{th,c}(t)$ demand. There are two sources that provide our system with electrical power, namely Germany's power grid, $P_{grid}(t)$, and the site's installed photovoltaic panels, $P_{pv}(t)$. The installation comprises PVs rated at $p_{pv}^{rPower} = 5$ megawatts (MW). The normalized maximum available power output for the PV system $v_{pv}(t)$ is illustrated in Figure 5 and was acquired using Meteonorm Software (Meteonorm, 2022). In this depicted system, the option for PV curtailment exists. For the sake of simplicity, curtailment costs are disregarded. Power procurement from the grid and the respective energy tariff contracts will be analysed in the next section. Additionally, the manufacturing site incorporates an ESU consisting of lithium-ion batteries with a combined capacity of $x_{el}^{rCapacity} =$ 12megawatt-hours (MWh) and a rated power of $p_{el,out/in}^{rPower} = 12$MW. Both the charging and discharging

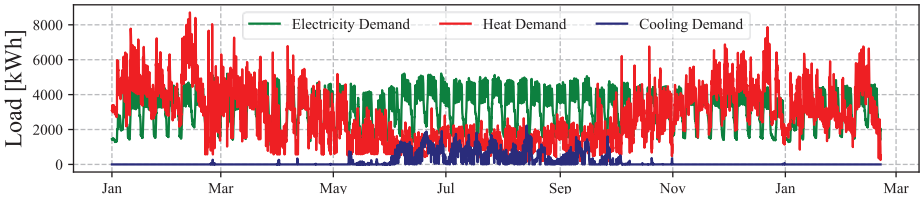

Figure 4: Load Demands

https://doi.org/10.52202/077185-0159

efficiencies are set at 94%, $\eta_{el}^{Ch} = \eta_{el}^{DCh} = 0.94$. Furthermore, losses attributed to the SOC of the battery are considered negligible, $\eta_{el}^{Self} = 0$. The site procures (natural) gas $P_{gas}(t)$ from Germany's gas grid. Within the scope of this paper, the gas price remains constant at $om_{gas} = 20$ cents per kilowatt-hour (kWh). A gas boiler combusts gas to elevate the temperature of the site's water to a specified level in degrees Celsius (°C) to fulfil its hot water requirements. For simplification purposes, the model does not include the water flow dynamics within the system. The boiler is characterized by a rated power output of $p_{boiler}^{rPower} = 8.5$ MW and operates with an efficiency of 85%, $\eta_{boiler}^{in} = 0.85$. Hot water provision is also facilitated by a heat pump system. Similar to the gas boiler, the water flow dynamics are not explicitly modelled in this analysis. The site's heat pump is characterized by a rated power of $p_{hp,th}^{rPower} = 5.4$ MW, and its COP $\eta_{hp}^{in}(t)$ (derived by measuring the outside temperature), concerning the thermal output relative to the electrical input, is illustrated in Figure 6. Furthermore, the site incorporates a hot water storage system with a capacity of $x_h^{rCapacity} = 6$ MWh and a rated power of $p_{h,in/out}^{rPower} = 4$ MW, enabling the storage of hot water for later utilization. The manufacturer also requires cold water for specific processes and building cooling purposes. This requirement is met through the utilization of an electric chiller with a rated power of $p_{chiller}^{rPower} = 2.4$ MW and a COP of 360%, $\eta_{chiller}^{in} = 3.6$. Additionally, a cold-water storage system with a capacity of $x_c^{rCapacity} = 2$ MWh and a rated power of $p_{c,in/out}^{rPower} = 1.8$ MW is employed, with charge and discharge efficiencies of 99%, $\eta_c^{Ch} = \eta_c^{Ch} = 0.99$ and minimal energy losses associated with its thermal energy level, namely $\eta_{el}^{Self} = 18 * 10^{-5}$.

2.3 Different Electric Energy Procurement Tariffs

There exist various energy procurement tariff structures, each designed to accommodate different operational and economic considerations. In our analysis, we will examine five distinct tariff models:

1. Baseline Tariff (BT): Under this tariff, energy procurement costs remain constant, fixed at 0.235€/kWh. This static pricing structure offers no price flexibility within the system, as the price remains unchanged irrespective of temporal or market conditions.
2. Spot Market Tariff (SMT): In this case, energy procurement costs are determined by the prevailing wholesale spot market prices observed in Germany during the year 2022. These prices fluctuate dynamically over time, reflecting the real-time supply and demand dynamics of the electricity market. As a result, dispatch controllers with varying optimization horizons will encounter differing levels of price flexibility. The time evolution of this tariffs is depicted in Figure 7.
3. Time of Use (ToU) Tariff: ToU tariffs introduce temporal variability into energy procurement costs, primarily governed by the time of day. Unlike spot market prices, which fluctuate continuously based on market dynamics, ToU tariffs delineate distinct periods throughout the day with varying electricity rates. Typically, these tariffs encompass a peak period characterized by heightened electricity demand and correspondingly elevated prices, alongside an off-peak period featuring significantly lower pricing. For analytical depth, we will utilize a ToU tariff comprising four distinct time periods: the base period, along with low, medium, and high peak periods, each associated with progressively incremental energy prices as showcased in Figure 7.

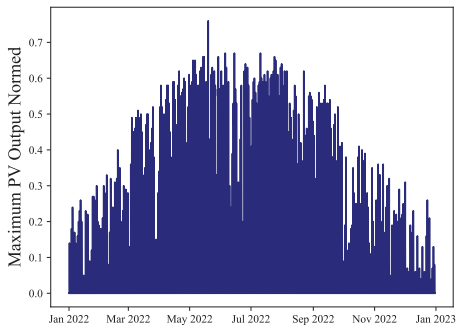

Figure 5: Maximum normalized available PV output $v_{pv}(t)$

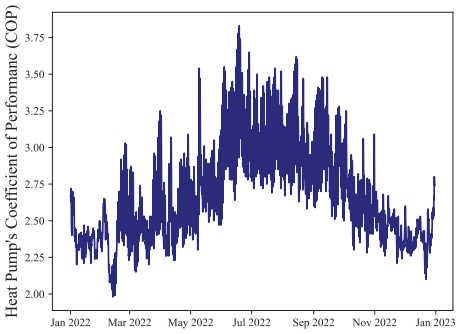

Figure 6: Heat Pump's COP.

https://doi.org/10.52202/077185-0159

In energy consuming industries, as the one considered here, commonly incur supplementary charges based on their monthly or annual peak loads (Berg and Savvides, 1983). In Germany, for instance, industries are subject to additional fees corresponding to the maximum power they draw from the grid over a period of one year. However, in order to add further temporal granularity in our dispatchers, we will use the monthly peak load components found in a neighbouring country, namely Switzerland. Expanding upon our tariff framework, we introduce two additional structures:

4. Spot Market Tariff with Monthly Peak Component (SMTwMPC): This tariff consists of the aforementioned SMT tariff with an extra monthly fee of 8.84€/kW, which is assessed based on the maximum power consumption from the grid observed within the respective month.
5. Time of Use with Monthly Peak Component (ToUwMPC): Again, this tariff is the same as the aforementioned ToU tariff but with an extra cost of 8.84€/kW for each monthly peak grid usage.

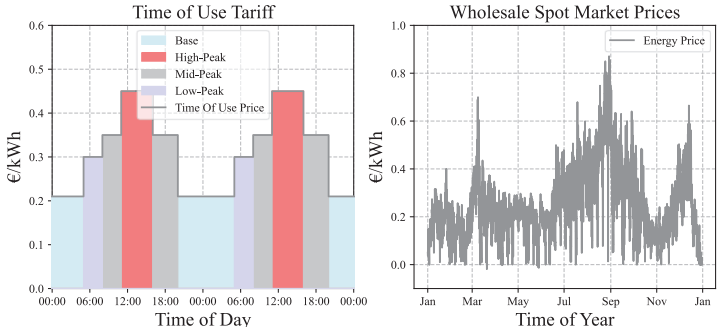

Figure 7: Energy procurement tariffs used in this research.

2.4 Assumptions and Parameters

Due to unavailability of 15minute data, we will resort to using hourly data, thereby adopting an hourly resolution. Nevertheless, the intended effects of interest will be still visible and present. Furthermore, European day-ahead prices have an hourly resolution (EpexSpot 2023) making our 1-hour resolution acceptable. We will employ a rolling horizon control strategy encompassing five distinct optimization horizons. The length of the optimization horizon will equal the controller's forecast horizon. Conversely, control horizon is set to $c_n = 1$ hour. The following optimization horizons are investigated:

- 365 Days: Perfect Foresight Dispatcher (PFD). The energy tariff values, along with weather and load data, are assumed to be fully known throughout the entire year (simulation period). While this scenario is unrealistic, it is commonly employed in sizing optimization scenarios. It will be demonstrated that relying on this assumption can yield overly optimistic outcomes. Nevertheless, this dispatcher offers us a lower limit for the minimum achievable operating costs of our system.
- 24 hours: 24Hours Dispatch (24HD). At each timestep, only the next 24 hours will be optimized. This resolution is usually used to schedule the unit commitment problems when the day ahead prices are known. Furthermore, during the dispatcher's 24 hours optimization horizon, even the biggest capacity to power ratio storage, the lithium-ion battery with a respective value of 10, can perform a whole charge-discharge cycle, giving the dispatcher a lot of flexibility.
- 12 hours: 12Hours Forecast (12HD). In this case, the optimization problem will be solved for 12 hours at each iteration. Compared to the 24-hours dispatcher, which could incorporate whole charging-discharging cycle times of all storages, this dispatcher has less flexibility but can still account for whole charging or discharging times of the lithium-ion battery.
- 4 hours: 4Hours Dispatcher (4HD). The optimization problem will be solved for 4 timesteps at each iteration.
- 1 hour: 1Hour Dispatcher (1HD). With a one-hour resolution, this dispatcher can be categorized as a single-step dispatcher. Such dispatchers are prevalent due to their independence from smart control mechanisms or prescient knowledge. At each step, they ensure power equilibrium is maintained in the most economically efficient manner possible.

https://doi.org/10.52202/077185-0159

3 Simulation and Results

All simulations are run on an i7-12800H 2.40GHz CPU with 32Gb Ram using SCIP optimizer (Bestuzheva, et al. 2021) as a solver for 8760 hourly timesteps (yearly simulation).

3.1 Case 0: No flexibility

First, the system is simulated with no energy flexibility. For that, consider the system described in 2.2 and depicted in Figure 1. We remove all storages and simulate the system with all dispatchers using the BT, SMT and ToU tariff. For each tariff, we obtain irrespective of the dispatcher's optimization horizon an annual operating cost of 7.249 million €, 8.250 million € and 10.494 million €, respectively. As expected, due to our perfect forecasts and the absence of any flexibility, the optimization horizon of our dispatcher does not have any effect on the resulting financial wins or system trajectories.

3.2 Case 1: Baseline Tariff

In this case, we add flexibility to our system by adding ESUs. First, we simulate our system using the baseline tariff where the electricity procurement price is constant. Table 1 shows the OPEX for the PFD as well as the increase in OPEX w.r.t the PFD for the rest of the dispatchers. Going from the PFD to the single-step dispatcher 1HD, the forecasted costs increase by a total of 0.39% which accounts for 28k€. The energy flexibility storages offer can capitalize on the temporal variability of energy prices, and through smart control procure the required energy quantities at lower costs. If, however, the energy costs are constant, the benefits of this flexibility diminish. On the other hand, the intermittent nature of solar power combined with energy storages can also act as a flexibility source. In this case, PFD, which has perfect knowledge of the future does not curtail any PV energy whereas 1HD curtails 1.06MWh.

Table 1: Operating costs for baseline tariff and different dispatchers

	Dispatcher				
	PFD	24HD	12HD	4HD	1HD
OPEX (€)	7.203.002	+0.02%	+0.05%	+0.28%	+0.39%

3.3 Case 2: Time-variant Tariffs

Compared to 3.2, we now add another source of flexibility through the time variability of electricity prices, which the ESUs can capitalize on. We simulate the system with the SMT and ToU tariffs. As seen in Table 2, for both time-sensitive tariffs, the optimization horizon's influence is greater than in 3.2. The projected operating costs of 1HD are 497.760€ and 738.796€ more than the PFD when using SMT and ToU tariffs, respectively. The ESUs have greater flexibility in choosing when to store or discharge energy. Figure 8 shows the equivalent full cycles of each storage based on their dispatcher and electricity tariff. Overall, the 24HD, which can account for the whole duration of the longest charge-discharge cycle, has almost identical full cycles with the PFD for all scenarios. Small differences may be attributed to the PFD's perfect knowledge of the whole year, which the 24HD lacks. A discontinuity in the cold water storage graph using ToU for the 4 HD case was detected, though its origin remains unknown. Figure 9 depicts the overall gas purchase in MWh. Smaller optimization horizons lead to increased purchase of gas. Specifically, compared to the PFD, 1HD buys 79% (64.7k €) and 63% (38.9k €) more gas from the gas grid. According to the German Federal Environment Agency (Umweltbundesamt, 2024) 202g of CO_2 are emitted per kWh gas consumed. Thus, going from a PFD to a 1HD dispatcher would result to 64.9 and 39.2 tonnes more forecasted CO_2 emissions using SMT and ToU, respective. Notice, however, that the cost function in (1) does not entail any emissions cost term, thus the CO_2 emissions of gas purchase are not directly penalized. PV curtailment is plotted in Figure 10.

Table 2: Operating costs for the SMT and ToU tariff and different dispatchers

		Dispatcher				
	Tariff	PFD	24HD	12HD	4HD	1HD
OPEX (€)	SMT	7.688.980	+0.065%	+0.64%	+2.78%	+6.47%
	ToU	9.726.521	+0.047%	+0.39%	+4.47%	+7.6%

https://doi.org/10.52202/077185-0159

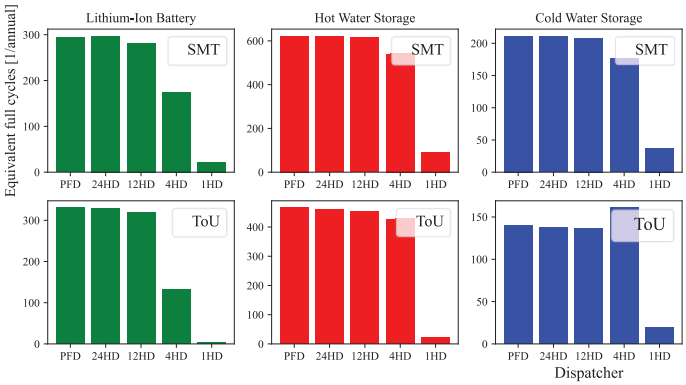

Figure 8: Full cycle of each storage [1/annual].

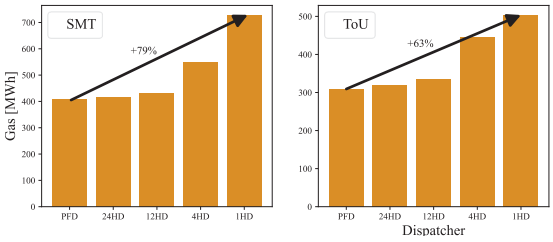

Figure 9: Gas Purchase [MWh]

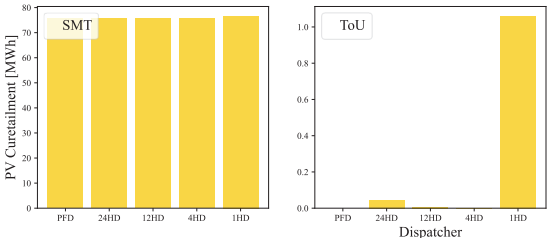

Figure 10: PV Curtailment [MWh]

Overall, it is evident that the energy flexibility provided by the systems' storages, the charging incentive and discharging costs of storages as well as the energy tariff structure and the dispatcher's optimization horizon strongly influence the anticipated financial and environmental benefits of an energy system design. Additionally, while not investigated in the scope of this research, it is pertinent to acknowledge, that the structure of the tariff utilized in each scenario also impacts the effects the optimization horizon has on the system (e.g., different PV curtailment motives in Figure 10).

3.4 Time-variant tariffs with monthly peak-load components

In this scenario, we simulate the system with the SMPwMPC and ToUwMPC tariffs. Table 3 displays the resulting OPEX costs. Again, it can be easily seen that shorter optimization horizons lead to greater operational costs. For example, the difference between the anticipated OPEX of PFD and 1HD for SMTwMPC and ToUwMPC is 590.641€ and 751.242€, respectively. The monthly peak load cost components of the yearly OPEX are displayed in Figure 11. In both scenarios, longer optimization horizons lead to greater monthly peak load cost components. However, the overall OPEX are smaller. This shows how longer optimization horizons can take advantage of their foresight and choose higher peak loads, that they can later make use of to burden the grid more at no additional cost. It is important to remember, that different heuristics my produce different results.

Table 3: Operating costs in case of monthly peak load components

		Dispatcher				
	Tariff	PFD	24HD	12HD	4HD	1HD
OPEX (€)	SMTwMPC	8.331.024	+0.8%	+1.48%	+3.53%	+7.09%
	ToUwMPC	10.405.359	+0.55%	+0.98%	+5.02%	+7.22%

4 Conclusion

Our goal is to demonstrate to prospective energy system designers the necessity to consider multiple factors when modelling energy systems and forecasting KPIs. Among those factors are the heuristic used for peak load management, the optimization horizon of the MPC, the energy procurement tariffs and the possible flexibility sources. We showcased the influence of each of the aforementioned factors on the projected KPIs. While seemingly minor, deviation of 7.6% in forecasted OPEX can substantially influence future investment decisions. Additionally, it becomes apparent, that substituting single-step

https://doi.org/10.52202/077185-0159

dispatchers with smart controllers that can leverage future insights and forecasts, holds considerable promise for reducing operating costs in industrial systems. Further research can focus on a more detailed analysis of the effects and synergies that exist between the energy procurement tariff structure and the energy system. Moreover, substituting ideal forecasts with more realistic erroneous forecasts and re-simulating our scenarios could yield intriguing findings and potentially greater disparities.

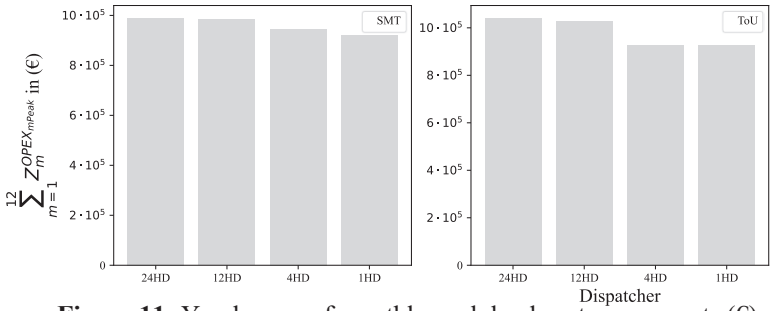

Figure 11: Yearly sum of monthly peak load cost components (€).

Nomenclature

$Z^{OPEX}(k)$	operating costs of energy procurement at optimization iteration k	(€)
$Z^{OPEX_{mPeak}}(k)$	monthly peak load costs at optimization iteration k	(€)
$om_{grid}(t)$	electricity price at timestep t	(€/kWh)
$om_{gas}(t)$	gas price at timestep t	(€/kWh)
om_{mPeak}	monthly peak load cost per kW	(€/kW)
p_i^{rPower}	installed rated input/output power of component i	(kW)
$X_i(t)$	energy content of storage component i at timestep t	(kWh)
$x_i^{rCapacity}$	rated installed capacity of storage component i	(kWh)
$P_{i,out}(t)$	power output of component i at timestep t	(kW)
$P_{i,in}$(t)	power input of component i at timestep t	(kW)
$w_q(t)$	heat ($q = th, h$), cooling ($q = th, c$), electric ($q = el$) load	(kW)
$v_{pv}(t)$	maximum normed available PV power ∈ [0,1] at timestep t	(-)
$\delta_i(t)$	binary variable that is 1 when storage i charges and 0 when it discharges	(-)
η_i^{Self}	self-discharge ∈ (0,1] of storage component i	(-)
η_i^{Ch}	charging efficiency ∈ (0,1] of storage component i	(-)
η_i^{Dch}	discharging efficiency ∈ (0,1] of storage component i	(-)
η_i^{in}	input-output efficiency ∈ (0,1] of component i	(-)
$\eta_{hp}^{in}(t)$	COP of component i at time-step t	(-)

Arguments

k	optimization iteration
t	timestep

Subscript

i	component indicator
m	month index ∈ {1,2,…,12}

References

AGEB. 2023. *Auswertungstabellen zur Energiebilanz Deutschland,* https://ag-energiebilanzen.de/daten-und-fakten/auswertungstabellen/.

Agha, M.H., Thery, R., Hetreux, G., Hait, A., and Le Lann, J.M., 2010, "Integrated production and utility system approach for optimizing industrial unit operations.", *Energy,* vol. 35, no. 2: p. 611-627.

Alarcón, M.A., Alarcón, R.G., González, A.H., and Ferramosca, A., 2022. "Economic model predictive control fosr energy management of a microgrid connected to the main electrical grid." *Journal of Process Control*, vol 117: p. 40-51.

https://doi.org/10.52202/077185-0159

Berg, S.V., and Savvides, A., 1983, "The theory of maximum kW demand charges for electricity.", *Energy Economics*, vol. 5, no. 4: p. 258-266.

Bestuzheva, K., Besançon, M., Chen, W.K., Chmiela, A., Donkiewicz, T., van Doornmalen, J., Eifler, L., and Gaul, O., 2021, *The SCIP Optimization Suite 8.0.*, Optimization Online, http://www.optimization-online.org/DB_HTML/2021/12/8728.html.

Bischi, A., Taccari, L., Martelli, E., Amaldi, E., Manzolini, G., Silva, P., Campanari, S., and Ennio Macchi. 2019. "A rolling-horizon optimization algorithm for the long term operational scheduling of cogeneration systems." *Energy*, vol.184: p. 73-90.

Cole, W.J., Edgar, T.F, and Novoselac, A., 2012, "Use of model predictive control to enhance the flexibility of thermal energy storage cooling systems." *ACC*, IEEE: p. 2788-2793.

EpexSpot, 2023, *Trading Products*, https://www.epexspot.com/en/tradingproducts.

Gupta, A., Saini, R.P., and Sharma, M.P., 2010, "Steady-state modelling of hybrid energy system for off grid electrification of cluster of villages.", *Renewable Energy*, vol. 35, no. 2: p. 520-535.

Hans, C.A., 2021, *Operation control of islanded microgrids*, Shaker Verlag, Berlin.

Leśko, M., Bujalski, W., and Futyma, K., 2018, "Operational optimization in district heating systems with the use of thermal energy storage.", *Energy*, vol. 165, no. A: p. 902-915.

Ma, J., Qin, J., Salsbury, T., Xu, P., 2012, "Demand reduction in building energy systems based on economic model predictive control.", *Chemical Engineering Science*, vol. 67, no.1: p. 92-100.

Ma, Q., Huang, x., Xu, C., Babaei, R., and Ahmadian, H., 2022, "Optimal sizing and feasibility analysis of grid-isolated renewable hybrid microgrids: Effects of energy management controllers.", *Energy*, vol.240: p. 122503.

Meteonorm Software 2022. https://meteonorm.com/

Mitra, S., Sun, L., and Grossmann, I.E., 2013, "Optimal scheduling of industrial combined heat and power plants under time-sensitive electricity prices.", *Energy*, vol. 54: p. 194-211.

Moretti, L., Polimeni, S., Meraldi, L., Raboni, P., Leva, S., and Manzolini, G., 2019, "Assessing the impact of a two-layer predictive dispatch algorithm on design and operation of off-grid hybrid microgrids.", *Renewable Energy*, vol. 143: p. 1439-1453.

Nassourou, M., Blesa, J., and Puig, V., 2020, "Optimal energy dispatch in a smart micro-grid system using economic model predictive control.", *Proceedings of the Institution of Mechanical Engineers, Part I: Journal of Systems and Control Engineering*, vol. 234, no. 1: p. 98-106.

Pérez-Piñeiro, D., Skogestad, S., and Boyd, S., 2023, "Home Energy Management with Dynamic Tariffs and Tiered Peak Power Charges." doi:10.48550/ARXIV.2307.07580.

Sawma, J., Khatounian, F., Monmasson, E., Ghosn, R., and Idkhajine, L., 2018, "The effect of prediction horizons in MPC for first order linear systems.", *2018 IEEE International Conference on Industrial Technology (ICIT)*, IEEE: p. 316-321.

Schreck, S., 2016, "Implementation and Analysis of a Rolling Horizon Approach for the Energy System Model REMix.", *Deutsches Zentrum für Luft- und Raumfahrt.*

Shezan, Sk.A., Fatin Ishraque, Md., Muyeen, S.M., Abu-Siada, A., Saidur, R., Ali, M.M, and Rashid, M.M., 2022, "Selection of the best dispatch strategy considering techno-economic and system stability analysis with optimal sizing.", *Energy Strategy Reviews*, vol.43: p. 100923.

Umwelt-Bundesamt. 2023. *Indicator: Greenhouse gas emissions in industry.* https://www.umweltbundesamt.de/en/data/environmental-indicators/indicator-greenhouse-gas-emissions-industry#at-a-glance.

Umwelt-Bundesamt. 2024. *Treibhausgas-Emissionen.* https://www.umweltbundesamt.de/themen/klima-energie/treibhausgas-emissionen.

Xu, Z., Han G., Liu, L., Martínez-García. M., and Wang, Z., 2021, "Multi-Energy Scheduling of an Industrial Integrated Energy System by Reinforcement Learning-Based Differential Evolution,.", *EEE Transactions on Green Communications and Networking*, vol. 5, no.3: p. 1077-1090.

Zhao, S., Maxim, A., Liu, S., De Keyser, R., and Ionescu, C., 2018, "Effect of Control Horizon in MPC for Steam/Water Loop in Large-Scale Ships.", *Processes*, vol. 6, no. 12, p: 265

Zhu, B., Tazvinga, H., and Xia, X., 2014, "Model Predictive Control for Energy Dispatch of a Photovoltaic-Diesel-Battery Hybrid Power System.", *IFAC Proceedings Volumes*, vol. 47, no. 3, p. 11135-11140.

 https://doi.org/10.52202/077185-0159